RESEARCH ARTICLE

ADVANCED
NANOBIOMED
RESEARCH
Open Access

www.advnanobiomedres.com

Surface Plasmon Resonance Assay for Label-Free and Selective Detection of *Xylella Fastidiosa*

Lucia Sarcina, Eleonora Macchia, Giuliana Loconsole, Giusy D'Attoma, Pasquale Saldarelli, Vito Elicio, Gerardo Palazzo, and Luisa Torsi*

Xylella fastidiosa **is among the most dangerous plant bacteria worldwide causing a variety of diseases, with huge economic impact on agriculture and environment. A surveillance tool, ensuring the highest possible sensitivity enabling the early detection of** *X. fastidiosa* **outbreaks, would be of paramount importance. So far, a variety of plant pathogen biomarkers are studied by means of surface plasmon resonance (SPR). Herein, multiparameter SPR (MP-SPR) is used for the first time to develop a reliable and label-free detection method for** *X. fastidiosa***. The real-time monitoring of the bioaffinity reactions is provided as well. Selectivity is guaranteed by biofunctionalizing the gold transducing interface with polyclonal antibodies for** *X. fastidiosa* **and it is assessed by means of a negative control experiment involving the nonbinding** *Paraburkholderia phytofirmans* **bacterium strain PsJN. Limit of detection of 10^5 CFU mL^{-1} is achieved by transducing the direct interaction between the bacterium and its affinity antibody. Moreover, the binding affinity between polyclonal antibodies and** *X. fastidiosa* **bacteria is also evaluated, returning an affinity constant of 3.5×10^7 m^{-1}, comparable with those given in the literature for bacteria detection against affinity antibodies.**

1. Introduction

The detection of pathogenic bacteria, virus, or fungi aimed at the identification of infectious plant disease is one of the most critical tasks in the monitoring of agriculture relevant species worldwide.[1] A relevant pathogen which stirred the interest of researchers in different countries is the bacterium *Xylella fastidiosa*. It is in fact one of the most dangerous plant bacteria worldwide, causing a variety of diseases, such as Pierce's disease of grapevine, phony peach disease, plum leaf scald, citrus variegated chlorosis disease, and olive scorch disease,[2,3] as well as leaf scorch on almond and on shade trees.[4] *X. fastidiosa* has been isolated from more than 300 plant species all over the world,[5,6] although not all of these plants are susceptible to disease.[7] *X. fastidiosa* is currently present in several European countries, mainly in Italy, France, and Spain,[8] where a number of areas are under eradication or containment strategies to avoid dissemination of this quarantine pest.[9] Eventually, international organizations, such as the European and Mediterranean Plant Protection Organization (EPPO), the International Plant Protection Convention of the Food and Agriculture Organization (IPPC-FAO), and the European Food Security Agency (EFSA), periodically release standards for diagnosis and detection of the pathogen, and update about the biology, epidemiology, and control of the bacterium.[10,11] They also provide the updated hosts' list, due to the continuous increase in new host species,[12] as well as the guidelines for plant tissue sampling.[13]

The transmission of the bacterium takes place through xylem-feeding vector insects that are widespread in the entire EU territory.[14] The spread of *X. fastidiosa* by insects does not require an incubation period in the vector that can acquire the bacterium by feeding on the xylem fluid of an infected plant and transmit it to healthy plants, immediately after acquisition. All this calls for strict control measures, to be taken immediately after any new outbreak is detected. Therefore, in this perspective a powerful surveillance tool, ensuring the highest possible level of early detection of outbreaks of *X. fastidiosa*, would be of paramount importance. The sooner the infection is identified the more effective the intervention on diseased trees can be. Therefore, the demand for sensors capable to detect plant pathogen with low

L. Sarcina, Prof. G. Palazzo, Prof. L. Torsi
Dipartimento di Chimica
Università degli Studi di Bari "Aldo Moro"
70125 Bari, Italy
E-mail: luisa.torsi@uniba.it

Dr. E. Macchia, Prof. L. Torsi
Faculty of Science and Engeneering
Åbo Akademi University
20500 Turku, Finland

Dr. G. Loconsole, Dr. G. D'Attoma, Dr. P. Saldarelli
Institute for Sustainable Plant Protection CNR
70124 Bari, Italy

V. Elicio
Agritest Srl, Tecnopolis Casamassima (BA)
70010, Italy

detection limits and selectivity is now increasing.[15] Several diagnostic protocols were tested for the detection of *X. fastidiosa*, such as enzyme-linked immunosorbent assay (ELISA),[16] polymerase chain reaction (PCR),[17,18] direct tissue blot immunoassay (DTBIA),[19] or loop-mediated isothermal amplification (LAMP).[20,21] The molecular amplification techniques currently available are very useful and play a key role in the preventive control and management of the disease.[10] Nevertheless, real-time PCR protocols involve a high cost per sample and require trained personnel. Moreover, cross-contamination among samples is a considerably important problem.[22] In this respect, highly selective and ultrasensitive immunological techniques could be very useful because of the reduced inhibitory effects from sample template contaminants as well as their suitability in large-scale testing.[23,24] Indeed, ELISA is a key technology for large monitoring programs due to easier management of large number of samples compared with genomic tests. Indeed, ELISA is the workhorse in the programs conducted in Italy, where more than 150 000 plants were tested from October 2017 to April 2018,[25] However, the limit of detection (LOD) of ELISA is at most of the order of 10^4 CFU mL^{-1}, while real-time PCR genomic detection goes down to about 10^2 CFU mL^{-1}.[26] However, these are all label-needing technologies. Namely, to measure the concentration of a given biomarker, a label (typically an enzyme) is needed to make the signal detectable. This increases the complexity of the overall assay procedures and adds steps and personnel cost to it, leading to a time-to-results of several hours. Therefore, the fast screening of plants that might be infected is difficult with such approaches. To this end, reliable point-of-care approaches need to be developed. They usually require a very stable layer of capturing antibodies that requires full characterization. One of the most suitable approaches in this respect is surface plasmon resonance (SPR) that is also a sensing technique on its own.

A wide variety of plant pathogen biomarkers were detected through SPR, with different degree of sensitivity depending on the assay configuration.[27–29] However, none of these studies involve *X. fastidiosa*. Among other techniques, SPR holds the advantage of being a label-free detection enabling also real-time monitoring of bioaffinity reactions. Indeed, the local variation of the surface refractive index can be directly correlated to the amount of bounded species, for which the interaction kinetics can also be determined.[30] Thus, the SPR platform is particularly useful not only as a detection method per se, but also for assessing the biofunctionalization protocol of gold surfaces with specific antibodies, validating their capturing efficacy against target analytes.[31] Therefore, it can be very useful to characterize an electrode that can be used for further development of biosensing

and bioelectronic methods. In fact, among the novel approaches, organic bioelectronic devices are of interest in many fields of application from clinical diagnostics[32–36] to agro-food,[33,37–39] and represent ideal candidates in point-of-care testing, due to low cost, rapidity, and portability.

The aim of the current study is to develop a multiparameter SPR (MP-SPR) study of a reliable and label-free detection method for *X. fastidiosa* achieving LODs comparable with the label-needing ELISA gold standard. Relevantly, to the best of our knowledge, the direct assay of *X. fastidiosa* with an SPR apparatus is here proposed for the first time. The system is also endowed with high selectivity by successfully functionalizing a gold transducing surface with the *X. fastidiosa* affinity antibodies. The selectivity is assessed by measuring the response of the nonbinding *Paraburkholderia phytofirmans* bacterium strain PsJN, which is a Gram-negative rod-shaped bacterium such as *X. fastidiosa*. The zero response over a wide range of concentrations proves the unprecedented selectivity of the assay toward *X. fastidiosa*. Moreover, the polyclonal antibodies and the *X. fastidiosa* bacteria affinity reaction binding constant, being 3.5×10^7 m^{-1}, have also been measured for the first time (**Table 1**).

2. Results and Discussion

2.1. SPR Sensor Surface Modification

One main requirement for a high-performing biosensors, and specifically immunoassay techniques, is the reproducibility of sensing surface, on which the biorecognition elements are immobilized. An effective method largely used in antibody-based sensors is the immobilization of these capturing antibodies on functional monolayers, whose terminal groups can be tailored for the required binding.[40] In the current work, gold sensor surfaces were modified by a self-assembly of alkylthiols with different chain length, prior to the amine coupling of polyclonal antibodies for the recognition of *X. fastidiosa* (anti-XF). An Au-coated (≈50 nm) SPR slides (BioNavis Ltd.) comprising a chromium adhesion layer (≈2 nm) served as semitransparent SPR substrate. To this aim, a mixed self-assembled monolayer (SAM) of 11-mercaptoundecanoic acid (11-MUA) and 3-mercaptopropionic acid (3-MPA), in a molar ratio of 1:10, was used as it was previously demonstrated to be particularly suited to achieve a very dense grafting of the capturing antibodies. The protocol is schematically shown in **Figure 1**. Indeed, a mixture of SAMs with different chain length is known to be preferable for large biomolecules effective immobilization because biomolecules are able to attach to the surface without undergoing

Table 1. Differences in performance between MP-SPR and state-of-the-art platforms for detection of *Xylella Fastidiosa*.

| Specification	ELISA[16]	rt-PCR[17,18]	DTBIA[19]	LAMP[20,21]	MP-SPR
Detection type	Quantitative	Qualitative	Qualitative	Qualitative	Quantitative
Limit of detection	10^5–10^4 CFU mL	10^2 CFU mL	10^3 CFU mL	10^2 CFU mL	10^5 CFU mL
Marker type	Proteins	Nucleic acids	Proteins	Nucleic acids	Proteins
Assay steps	5	4	2	2	2
Label-needing	Yes	Yes	Yes	Yes	No
Assay time	At least 5 h	2–5 h	<1 h	20 min	<1 h
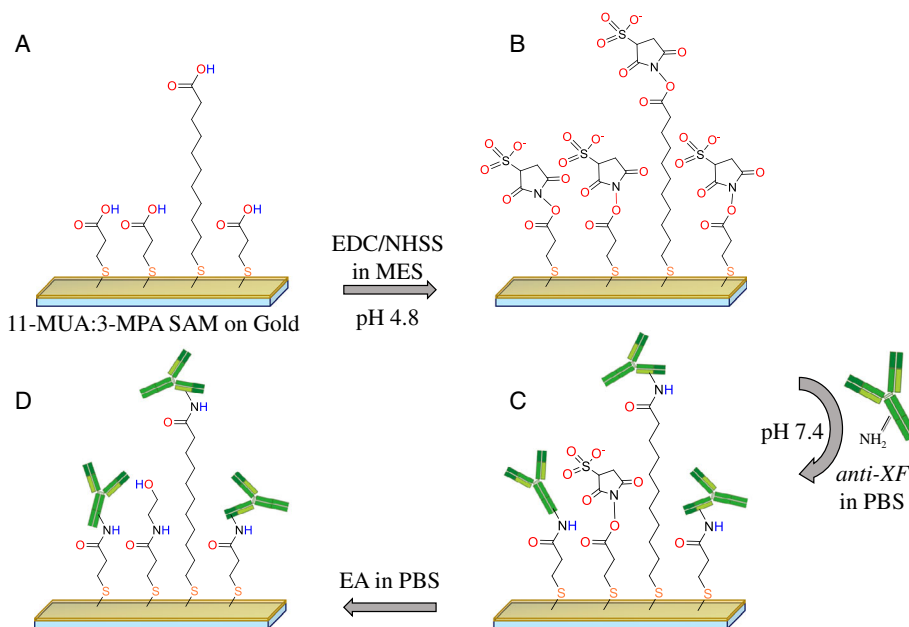
Figure 1. Diagram of the functionalization procedure conducted and detected with the SPR. A) SAM formation on the gold surface; B) activation of the terminal groups of alkanethiols through EDC/NHSS coupling; C) anchoring of the anti-XF antibodies (not in scale) to the SAM; and D) deactivation of unreacted sites with EA.

conformational changes due to steric hindrance and therefore an enhanced surface coverage of functional proteins can be obtained.[41–43] More in detail the protocol involved the activation of carboxyl terminal groups of alkylthiols through 1-ethyl-3-(3-dimethylamino-propyl)carbodiimide (EDC)/*N*-hydroxysulfosuccinimide sodium salt (NHSS) (0.2 m/0.05 m) coupling,[44] in a 2-(*N*-morpholino)ethane-sulfonic acid (MES) buffer at controlled pH 4.8 (Figure 1A,B). Then, the surface was rinsed with phosphate buffer solution (PBS) at pH 7.4 and further exposed to the anti-XF buffer solution at a concentration of $10 \mu g\,mL^{-1}$ (Figure 1C). In addition to a solution of ethanolamine (EA), 1 m was used to saturate possible unreacted esters on the

SAM. The scheme of the final modified sensor surface is shown in Figure 1D.

The SPR apparatus allowed the real-time monitoring of each step of the binding process, by measuring the angular variation of the plasmon peak minimum versus time, as shown in the sensogram spectrum reported in **Figure 2**A. The functionalization was performed by manual injections of each reagent, in a $100 \mu L$ single channel cell. The gold exposed area of about $0.4 \, cm^2$ was sampled simultaneously into two different points with two laser beams at wavelength of 670 nm. The two traces, shown as red and blue curves in Figure 2, give an idea of the high homogeneity of the layer. Once the sensor was placed in the
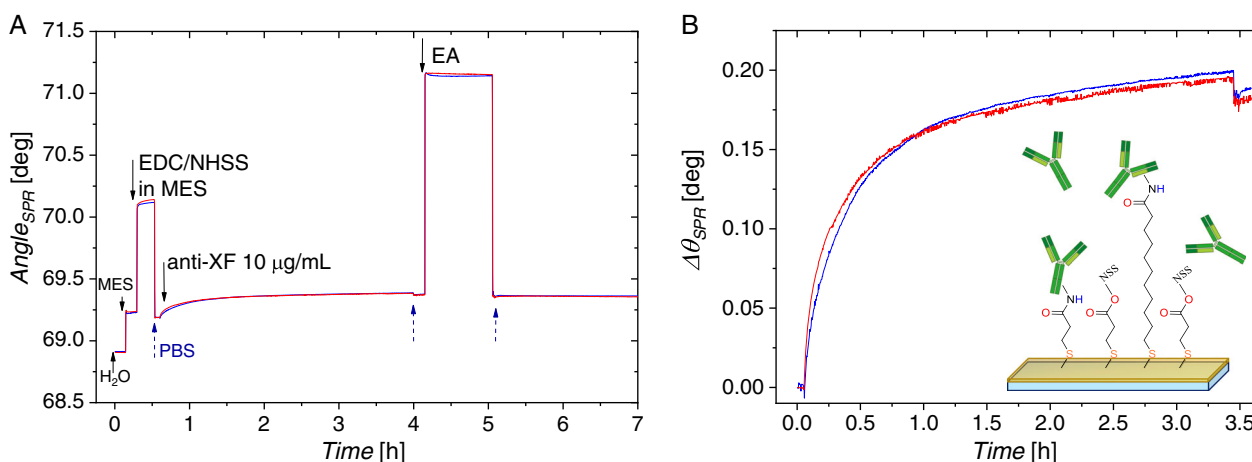

Figure 2. A) Sensogram of the functionalization protocol. Red and blue curves are the signals measured on the two different inspected areas of the sensing surface. Black arrows correspond to the injection of each solution, while blue dotted arrows indicate surface rinsing with the buffer solution. B) Angle shift ($\Delta\theta_{SPR}$) versus time of the real-time anchoring of anti-XF from a $10 \mu g\,mL^{-1}$ solution in PBS.

**ADVANCED
SCIENCE NEWS**
www.advancedsciencenews.com

**ADVANCED
NANOBIOMED
RESEARCH**
Open Access
www.advnanobiomedres.com

sample-holder, the surface was rinsed with water and MES until a stable trace was measured that was taken as the baseline. Then, the EDC/NHSS solution in MES was injected and kept in contact with the sensor for 15 min. The variation of surface refractive index produces the SPR angle change observed in the sensogram. Then, the PBS solution was injected, and a new stable baseline was acquired before injecting the PBS solution of the anti-XF to be bound on the SAM. Figure 2B shows the anti-XF grafting that is completed in 3.5 h, when the trace levels off. After PBS rinsing, the EA solution was injected and kept in contact with the sensing area for 45 min. Finally, PBS was injected to rinse the surface and remove not covalently bound species. The angle shift ($\Delta\theta_{SPR}$) recorded starting from the initial PBS baseline to the final rinsing after EA represents the amount of effectively bound antibodies.[45]

The elicited protocol leads to a very dense layer of the anti-XF with a minimal consumption of regents due to the optimization of the method previously performed.[46,47] Indeed, by using the MES buffer at pH 4.8, more efficient reactions between the EDC/NHSS and the carboxyl terminal groups can be obtained.[45,48] Then, for the reaction with the activated esters (NSS) to occur, the antibody needs to be brought in close proximity with the surface, promoting the electrostatic attraction with the oppositely charged remaining surface carboxyls.[45] Two factors should be considered in the antibody biding reaction: the charge on its amino groups could be kept positive if the pH is 0.5–1 units below the isoelectric point (pI) of the antibody, and the negative charge of the carboxyl groups on the sensor surface could be preserved by a surface pH above 4. Therefore, a two-step immobilization protocol has been chosen to fit the best experimental condition, in which the MES buffer is replaced by PBS at pH 7.4 before injecting the solution of antibodies (p $\approx$7/8).[49] Indeed, by using 100 μL of an anti-XF 10 μg mL^{-1} solution in PBS, an average angle shift $\Delta\theta = (0.16 \pm 0.04)$ degree was recorded for ten replicate measurements. This SPR angle variation was used to calculate the surface coverage of the biorecognition element by means of the de Feijter's Equation (1)

$$\Gamma = d \times (n - n_0) \times \left(\frac{dn}{dC}\right)^{-1} \quad (1)$$

The surface coverage (Γ, expressed in ng cm^{-2}) is proportional to the thickness of the deposited ligand (d), to the difference in refractive index of the adlayer (n) and the bulk medium (n_0), and to the refractive index increment (dn/dC). Moreover, the instrument response is correlated to the refractive index variation by the equation

$$(n - n_0) = \Delta\theta_{SPR} \times k \quad (2)$$

where k is the wavelength-dependent sensitivity coefficient, and $\Delta\theta_{SPR}$ is the measured angular shift. For a thin layer (<100 nm) and at a $\lambda = 670$ nm, the ratio dn/dC is approximated to 0.182 cm^3 g^{-1}, whereas $k \cdot d \approx 1.0 \times 10^{-7}$ cm degree^{-1};[50] thus by introducing Equation (2) into Equation (1), the surface coverage can be estimated as

$$\Gamma = \Delta\theta_{SPR} \times 550 \text{ [ng cm}^{-2}] \quad (3)$$

Table 2. Summary of the SPR angle shift ($\Delta\theta_{SPR}$) recorded after antibodies anchoring and EA bounds' saturation. The reported angle shifts are measured after PBS washing, depicted as blue dotted arrows in figure 2a, along with the corresponding surface coverages.

Steps	Time [h]	$\Delta\theta_{SPR}$ [deg]	Surface coverage [ng cm^{-2}]	Surface coverage [molecules cm^{-2}]
Anti-XF (after PBS)	4	0.17 ± 0.04	97 ± 20	(3.9 ± 0.8) × 10^{11}
Anti-XF (after EA/PBS)	5	0.16 ± 0.04	89 ± 21	(3.6 ± 0.8) × 10^{11}

In **Table 2**, the experimental angle shift measured after anti-XF binding and after the saturation with EA is given along with the surface coverages estimated from Equation (3). The antibody surface coverage is as high as 89 ± 21 ng cm^{-2}, corresponding to (3.6 ± 0.8) × 10^{11} molecules cm^{-2}. This represents a homogeneous layer of densely packed biorecognition elements, which provides a highly packed transducing surface for the interaction with the target species.[47]

The response registered for the antibody coverage in this study was comparable with those reported in the literature, with equivalent working conditions, for which an angular response of $\Delta\theta_{SPR} \approx 0.18°$ was recorded.[51,52] The error bars have been estimated as the relative standard deviation of the surface coverages on two different replicates and four different sampled areas, to provide an estimation of the homogeneity of the biolayer uniformity. Indeed, SPR sensograms were acquired from four different points on two different SPR slides.

2.2. SPR Assay of *Xylella Fastidiosa*

To the best of our knowledge, the direct assay of *X. fastidiosa* with SPR has been performed for the first time. Indeed, the SPR direct assay configuration for large cell detection, such as bacteria, has been very seldom investigated, due to its limited sensitivity of direct cell capture.[51] In fact, one of the major limiting factors in SPR assay is represented by the fluid forces that have to be overcome before particles can reach the sensor surface where they are captured.[52] Once cells have found their target, the antibody–cell-binding affinity must be able to withstand the effect of those forces, generated by the laminar flow of the SPR apparatus. Remarkably, in the current work, SPR configuration has been optimized to overcome this main limitation. Indeed, the *X. fastidiosa* direct assay has been performed operating the SPR sensor in static conditions, preventing the effect of any fluid forces. Moreover, the optimized SPR cell is endowed with a wide field sensing area. Therefore, the high density of anchored antibodies on the cm^2 area allowed to enhance the capturing efficiency of the detecting interface toward the target bacteria. The biofunctionalized SPR sensor slide was tested against the specific binding of the *X. fastidiosa* in a range of concentration from 10^5 to 2 × 10^8 CFU mL^{-1}. The relevant sensogram is shown in **Figure 3**.

The assay was conducted by injecting *X. fastidiosa* solutions in PBS at different concentrations. Each solution was let to interact with the anti-XF functionalized interface for 40 min (Figure 3A), minimum time required to reach the equilibrium between bounded species at the surface and unbounded bacteria in
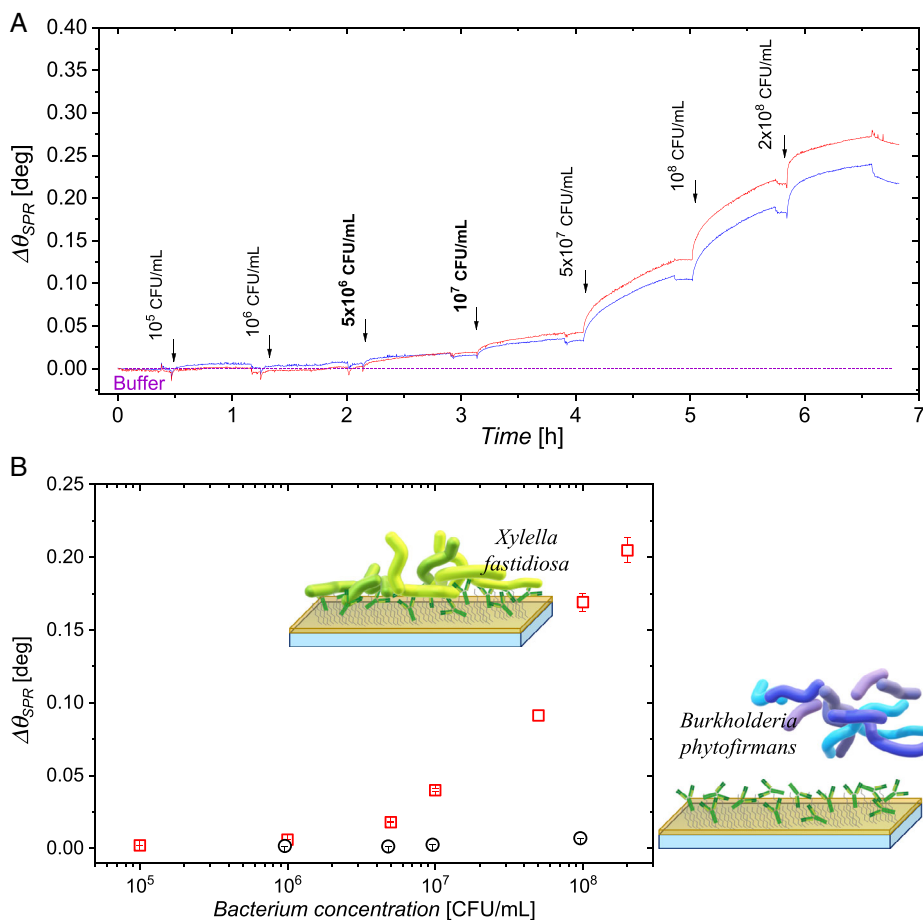
**ADVANCED
SCIENCE NEWS**

www.advancedsciencenews.com

**ADVANCED
NANOBIOMED
RESEARCH**
Open Access

www.advnanobiomedres.com

Figure 3. A) Exposure of the anti-XF functionalized surface to *X. fastidiosa* at increasing concentrations; black arrows correspond to sample injections and purple dotted line refers to the buffer level. Red and blue lines refer to two sampling points measured simultaneously. B) Comparison of *X. fastidiosa* (red square) and *Burkholderia phytofirmans* (black circle) SPR responses against the anti-XF functionalized surface. The average signal and standard deviation for four replicates analysis are reported.

solution. Upon equilibrium, the bacterium excess was removed by rinsing with the PBS buffer solution. The signal after each rinsing was compared with the initial baseline, acquired in PBS buffer solution, taken as the zero-level signal in the sensogram. Also in this case, the exposed sensing area was sampled in two different points (blue and red signal in Figure 3A). The SPR data reported as red squares in Figure 3B are the averages over three replicates, for which a relative standard deviation, RSD, of 1% was computed. Relevantly all the analysis was performed at controlled temperature, due to the dependency of the refractive index from temperature changes.[43] Indeed, the MP-SPR used in this study is equipped with a thermostatic apparatus that was set at room temperature, to avoid any discrepancy between the temperature value of SPR sensor surface and the solution injected.

The selectivity of the assay was evaluated by exposing the sensing interface to a nonbinding species. To this end, the interaction of the anti-XF functionalized surface with the *P. phytofirmans* strain PsJN, a Gram-negative bacterium was assayed. The SPR angle shift versus the *P. phytofirmans* concentration is reported in Figure 3B as black circle. The selectivity of the biosensing platform has been successfully demonstrated, as the negative

control experiment involving the *P. phytofirmans* showed a maximum angle shift below 0.01°, being only 4% of the signal registered for the *X. fastidiosa* assay. Therefore, although some spurious nonspecific adsorption could not be ruled out considering the aggregating nature of these bacteria,[6] the major contribution to the SPR signal can be ascribed to the binding between *X. fastidiosa* and its specific antibodies. Thus, the selectivity of the assay was estimated as the ratio between the angle-shift measured for *P. phytofirmans* and *X. fastidiosa*, respectively, resulting in a value as low as $\Delta\theta_{\text{BPhy}}/\Delta\theta_{\text{XF}} = 0.05 \pm 0.01$. This is among the lowest measured values as the closest best is as high as 0.23.[26,53,54]

The LOD of the assay was evaluated considering the linear portion of the calibration curve, as shown in Figure 3. To this aim, the linear regression on the data of angle shift versus analyte concentration was reported in Figure S1, Supporting Information. The fit of the linear portion of the curve (highlighted range 10^5–10^7 CFU mL^{-1}) is given as a red dotted line in Figure S1, Supporting Information. In the same figure, the black circles are the data coming from the negative control experiment involving the *P. phytofirmans* bacterium assay, and the black dotted line

**ADVANCED
SCIENCE NEWS**
www.advancedsciencenews.com

**ADVANCED
NANOBIOMED
RESEARCH**
Open Access
www.advnanobiomedres.com

is its average signal (s_C). The LOD was evaluated as the average signal of the negative control experiment (s_C) plus three times its standard deviation (σ_C). This level is therefore $\gamma = s_C + 3\sigma_C = 3.18 \times 10^{-3}$ degree. The comparison of this level with the interpolating linear regression results in a LOD of $(3.3 \pm 0.2) \times 10^5$ CFU mL^{-1}. This well compares with the detection limit found with SPR for different bacteria species in similar test conditions, as well as with ELISA gold standard.[51,55] Indeed, the signal-to-noise ratio of the SPR apparatus is not sufficiently high to detect bacteria concentrations below 10^4 CFU mL^{-1}.[56–58] On the contrary, the maximum bacteria concentration assayed was 2×10^8 CFU mL^{-1}, corresponding to the concentration needed to fully cover the biofunctionalized sensing surface. The latter has been estimated considering the number of X. fastidiosa covering the 0.4 cm^2 wide gold area, evaluating the bacteria footprint as rod-like shaped capsules, with radius of 0.25 μm and an end-to-end length of 1.90 μm.[2,53,54,59]

To complete the characterization, the binding affinity equilibrium constants were also evaluated with SPR using a nonregenerative approach.[60] Indeed, surface regeneration between consecutive analyte injections to remove the bound analytes cannot be used in case of stable ligand–analyte complexes, such as antibodies–bacteria binding interactions, where the dissociation binding-pairs rate (k_{off}) falls in the range of 10^{-4} s^{-1}.[61] In fact, with such systems the regeneration may fail in removing all the bound analyte molecules; as a result, the SPR signal would not be close enough to the baseline after the regeneration. Moreover, harsh regeneration reagents may destroy the bioactivity of the ligand molecules. Consequently, a nonregenerative approach has been proposed herein to investigate the interaction kinetics between the X. fastidiosa and its affinity antibody. To this aim, a clean gold sensor surface was allocated in the SPR apparatus and exposed to a 2×10^8 CFU mL^{-1} concentration of X. fastidiosa for 50 min to deposit a layer of the bacterium. As shown in Figure S2, Supporting Information, the angle shift was $\Delta\theta = 0.149° \pm 0.001°$. Then, anti-XF solutions at increasing concentration (in the 10–100 nM range) were injected and let to stay in contact with the bacteria film for 40 min, each.

The dependence of the SPR response from the concentration can be described, once the equilibrium is reached on the binding surface, by Equation (5)[60]

$$k_{on} \cdot [\text{anti} - \text{XF}] \cdot (\Delta\theta_{max} - \Delta\theta_{eq}) = k_{off}\Delta\theta_{eq} \quad (4)$$

or equivalently

$$\frac{1}{\Delta\theta_{eq}} = \frac{1}{\Delta\theta_{max}} + \frac{1}{K_A\Delta\theta_{max}} \cdot \frac{1}{[\text{anti} - \text{XF}]} \quad (5)$$

where k_{on} and k_{off} are the association and dissociation binding-pairs rate, respectively, [anti-XF] is the antibody concentration, $\Delta\theta_{eq}$ is the angle shift measured at equilibrium after association at each concentration, $\Delta\theta_{max}$ the highest angle shift at signal saturation, and K_A is the affinity constant defined as k_{on}/k_{off}. By plotting $1/\Delta\theta_{eq}$ [deg^{-1}] versus 1/anti-XF [M^{-1}] as shown in Figure S3, Supporting Information, the values for the maximum SPR response and the affinity constant (K_A) of the species can be calculated from the intercept and slope of the linear fit. The resulting K_A value obtained is 3.5×10^7 m^{-1}, which is comparable with the affinity constant value found in works for bacteria detection by antibodies, with comparable testing conditions.[61,62]

3. Conclusions

The SPR platform has been herein proposed for the first time as a label-free, fast, and reliable detection method for X. fastidiosa, achieving LOD comparable with the label-needing ELISA gold standard (10^5 CFU mL^{-1}). Moreover, SPR has been proposed as powerful tool to assess the optimized biofunctionalization protocol of gold surfaces with anti-XF, validating their capturing efficacy against X. fastidiosa. The selectivity of the sensor surface has been assessed as well, by comparing the cross-reactivity of the P. phytofirmans nonbinding bacterium strain PsJn, showing unprecedented performance in both sensor stability and selectivity. Moreover, the binding affinity between anti-XF and the X. fastidiosa bacteria has also been tested in the SPR apparatus, obtaining an affinity constant value comparable with those reported in the literature for bacteria detection with antibody/antigen assays. Remarkably, the SPR platform hereby presented paves the way for further development of a wide-field bioelectronic sensor, to accomplish an efficient presymptomatic diagnosis of diseases caused by X. fastidiosa. In fact, diagnostic tools for early detection of X. fastidiosa are urgently required. Indeed, such goal relies on the capability to obtain stable biofunctionalized gold transducing interface with purified immunoglobulin (IgG) selective for X. fastidiosa. As a future perspective, the reliable and cost-effective biofunctionalization protocol developed herein will be used to immobilize trillions of anti-XF antibodies on the gold gate electrode of an electrolyte-gated field effect transistor, to achieve ultrasensitive and selective detection of X. fastidiosa.

4. Experimental Section

3-Mercaptopropionic acid (3MPA) (98%), 11-mercaptoundecanoic acid (11MUA), ethanolamine hydrochloride (EA), EDC, NHSS, and bovine serum albumin (BSA, molecular weight 66 kDa) were purchased from Sigma-Aldrich and used without further purification. Phosphate-buffered saline was purchased from Sigma-Aldrich. The PBS composition for sensor modification contains phosphate buffer 0.01 M, KCl 0.0027 M, NaCl 0.137 M tablet dissolved in 200 mL HPLC water and used upon filtration on Corning 0.22 μm polyethersulfone membrane; the buffer obtained is at pH 7.4. The buffer used for bacteria dilution (NaH$_2$PO$_4$ 0.020 M, NaCl 0.5%) was adjusted at pH to 6.8 by KOH before autoclaving. MES (Sigma-Aldrich) was prepared at 0.1 m buffer solution and adjusted at pH 4.8–4.9 with sodium hydroxide solution (NaOH 1 M). SPR glass sensor slides (SPR Navi-200) coated with 50 nm gold layer were used after deep cleaning in a NH$_4$OH/H$_2$O$_2$ aqueous solution (1:1:5 v v^{-1}) at 80–90 °C for 10 min. Slides were then rinsed in water, dried with nitrogen and treated for 10 min in an UV-ozone cleaner. Substrates were immersed in a 10 mM thiol solution 11-MUA: 3-MPA (1:10 molar ratio) in degassed ethanol and left overnight in nitrogen atmosphere at 25 °C. Samples were rinsed with ethanol and water prior to the location in the SPR sample-holder. A BioNavis MP-SPR NaviTM instrument, in the Kretschmann configuration, was used. All the experiments were performed at 24 °C. For the analysis of SPR data, an Origin2018 graphing software by OriginLab Corporation was used.

Ten-day-old colonies of X. fastidiosa, subsp. pauca De Donno strain, sequence-type ST53 and 2-day-old colonies of P. phytofirmans PsJN were

**ADVANCED
SCIENCE NEWS**

www.advancedsciencenews.com

**ADVANCED
NANOBIOMED
RESEARCH**
Open Access

www.advnanobiomedres.com

scraped from plates and dispersed in sterile potassium phosphate buffer (0.05 M, pH 7.2) to prepare tenfold serial dilutions. Bacterial cells concentrated from 10^8 to 10^4 CFU mL^{-1} were tested for both bacteria. The effective bacteria concentrations, expressed in CFU mL^{-1}, were determined using plate count as the reference method. Specifically, the dilutions used were: $(2 \times 10^8; 10^8; 5 \times 10^7; 10^7; 5 \times 10^6; 10^6; 10^5)$ CFU mL^{-1}. Purified-IgG against *X. fastidiosa* (analytical specificity validated by EPPO standard) at concentration of 1 mg mL^{-1} was provided by Agritest and diluted to 10 μg mL^{-1}.

Supporting Information

Supporting Information is available from the Wiley Online Library or from the author.

Conflict of Interest

The authors declare no conflict of interest.

Data Availability Statement

The data that support the findings of this study are available on request from the corresponding author. The data are not publicly available due to privacy or ethical restrictions.

[1] P. K. Anderson, A. A. Cunningham, N. G. Patel, F. J. Morales, P. R. Epstein, P. Daszak, *Trends Ecol. Evol.* **2004**, *19*, 535.

[2] C. Cariddi, M. Saponari, D. Boscia, A. De Stradis, G. Loconsole, F. Nigro, F. Porcelli, O. Potere, G. P. Martelli, *J. Plant Pathol.* **2014**, *96*, 425.

[3] T. Elbeaino, F. Valentini, R. Abou Kubaa, P. Moubarak, T. Yaseen, M. Digiaro, *Phytopathol. Mediterr.* **2014**, *53*, 533.

[4] N. B. Pierce, *U.S. Dep. Agric. Div. Veg. Pathol. Bull.* **1892**, *2*, 222.

[5] P. Baldi, N. La Porta, *Front. Plant Sci.* **2017**, *8*, 944.

[6] G. S. Lorite, A. A. de Souza, D. Neubauer, B. Mizaikoff, C. Kranz, M. A. Cotta, *Colloids Surf. B Biointerfaces* **2013**, *102*, 519.

[7] EPPO, *PM1002(29) EPPO A1 and A2 Lists of Pests Recommended for Regulation as Quarantine Pests*, EPPO, Paris (France), **2020**.

[8] B. B. Landa, A. I. Castillo, A. Giampetruzzi, A. Kahn, M. Román-Écija, M. P. Velasco-Amo, J. A. Navas-Cortés, E. Marco-Noales, S. Barbé, E. Moralejo, H. D. Coletta-Filho, P. Saldarelli, M. Saponari, R. P. P. Almeida, *Appl. Environ. Microbiol.* **2020**, *86*, 1.

[9] European Commission, *Off. J. Eur. Union* **2020**, *1201*, 2.

[10] EPPO *EPPO Bull.* **2019**, *49*, 175.

[11] IPPC-FAO, *Int. Stand. Phytosanitary Meas.* **2018**, ISPM 27, DP 25.

[12] EFSA (European Food Safety Authority), *EFSA J.* **2020**, *18*, 6114.

[13] EFSA (European Food Safety Authority), E. Lázaro, S. Parnell, A. Vicent Civera, J. Schans, M. Schenk, G. Schrader, J. Cortiñas Abrahantes, G. Zancanaro, S. Vos, *EFSA Support. Publ.* **2020**, *76*.

[14] EFSA (European Food Safety Authority), S. Vos, M. Camilleri, M. Diakaki, E. Lázaro, S. Parnell, M. Schenk, G. Schrader, A. Vicent, *EFSA Support. Publ.* **2019**, *52*.

[15] M. Khater, A. de la Escosura-Muñiz, A. Merkoçi, *Biosens. Bioelectron.* **2017**, *93*, 72.

[16] G. Loconsole, O. Potere, D. Boscia, G. Altamura, K. Djelouah, T. Elbeaino, D. Frasheri, D. Lorusso, F. Palmisano, P. Pollastro, M. R. Silletti, N. Trisciuzzi, F. Valentini, V. Savino, M. Saponari, *J. Plant Pathol.* **2014**, *96*, 7.

[17] G. V. Minsavage, C. M. Thompson, D. L. Hopkins, R. M. V. B. C. Leite, R. E. Stall, *Phytopathology* **1994**, *84*, 456.

[18] W. Guan, J. Shao, T. Elbeaino, R. E. Davis, T. Zhao, Q. Huang, *PLoS One* **2015**, *10*, 0129330.

[19] K. Djelouah, D. Frasheri, F. Valentini, A. M. D'Onghia, M. Digiaro, *Phytopathol. Mediterr.* **2014**, *53*, 559.

[20] S. J. Harper, L. I. Ward, G. R. G. Clover, *Phytopathology* **2010**, *100*, 1282.

[21] T. Yaseen, S. Drago, F. Valentini, T. Elbeaino, G. Stampone, M. Digiaro, A. M. D'Onghia, *Phytopathol. Mediterr.* **2015**, *54*, 488.

[22] S. H. De Boer, M. M. López, *Annu. Rev. Phytopathol.* **2011**, *50*, 197.

[23] D. Boscia, A. Myrta, *Options Mediterr. Ser. B Etudes Rech.* **1998**, *19*, 171.

[24] M. Cambra, D. Boscia, M. Gil, E. Bertolini, A. Olmos, in *Virus Virus-Like Dis. Pome Stone Fruits* (Eds.: A. Hadidi, , M. Barba, T. Candresse, W. Jelkmann), The American Phytopathological Society, Saint Paul, MN **2011**, pp. 303–313.

[25] M. Saponari, G. D'Attoma, R. Abou Kubaa, G. Loconsole, G. Altamura, S. Zicca, D. Rizzo, D. Boscia, *Eur. J. Plant Pathol.* **2019**, *154*, 1195.

[26] S. Waliullah, O. Hudson, J. E. Oliver, P. M. Brannen, P. Ji, M. E. Ali, *PLoS One* **2019**, *14*, 0221903.

[27] T. Candresse, H. Lot, S. German-Retana, R. Krause-Sakate, J. Thomas, S. Souche, T. Delaunay, M. Lanneau, O. Le Gall, *J. Gen. Virol.* **2007**, *88*, 2605.

[28] G. Lautner, Z. Balogh, V. Bardóczy, T. Mészáros, R. E. Gyurcsányi, *Analyst* **2010**, *135*, 918.

[29] A. D. Taylor, J. Ladd, Q. Yu, S. Chen, J. Homola, S. Jiang, *Biosens. Bioelectron.* **2006**, *22*, 752.

[30] V. Nanduri, A. K. Bhunia, S. I. Tu, G. C. Paoli, J. D. Brewster, *Biosens. Bioelectron.* **2007**, *23*, 248.

[31] M. J. Linman, A. Abbas, Q. Cheng, *Analyst* **2010**, *135*, 2759.

[32] E. Macchia, K. Manoli, B. Holzer, C. Di Franco, M. Ghittorelli, F. Torricelli, D. Alberga, G. F. Mangiatordi, G. Palazzo, G. Scamarcio, L. Torsi, *Nat. Commun.* **2018**, *9*, 3223.

**ADVANCED
SCIENCE NEWS**

www.advancedsciencenews.com

**ADVANCED
NANOBIOMED
RESEARCH**
Open Access

www.advnanobiomedres.com

[33] E. Macchia, L. Sarcina, R. A. Picca, K. Manoli, C. Di Franco, G. Scamarcio, L. Torsi, *Anal. Bioanal. Chem.* **2020**, *412*, 811.

[34] E. Macchia, K. Manoli, C. Di Franco, R. Picca, R. Osterbacka, G. Palazzo, F. Torricelli, G. Scamarcio, L. Torsi, *ACS Sensors* **2020**, *5*, 1822.

[35] E. Macchia, K. Manoli, B. Holzer, C. Di Franco, R. A. Picca, N. Cioffi, G. Scamarcio, G. Palazzo, L. Torsi, *Anal. Bioanal. Chem.* **2019**, *411*, 4899.

[36] E. Macchia, A. Tiwari, K. Manoli, B. Holzer, N. Ditaranto, R. A. Picca, N. Cioffi, C. Di Franco, G. Scamarcio, G. Palazzo, L. Torsi, *Chem. Mater.* **2019**, *31*, 6476.

[37] E. Primiceri, M. S. Chiriacò, F. de Feo, E. Santovito, V. Fusco, G. Maruccio, *Anal. Methods* **2016**, *8*, 3055.

[38] E. Macchia, R. A. Picca, K. Manoli, C. Di Franco, D. Blasi, L. Sarcina, N. Ditaranto, N. Cioffi, R. Österbacka, G. Scamarcio, F. Torricelli, L. Torsi, *Mater. Horizons* **2020**, *7*, 999.

[39] M. S. Chiriacò, E. Primiceri, F. De Feo, A. Montanaro, A. G. Monteduro, A. Tinelli, M. Megha, D. Carati, G. Maruccio, *Biosens. Bioelectron.* **2016**, *79*, 9.

[40] C. Nicosia, J. Huskens, *Mater. Horizons* **2014**, *1*, 32.

[41] J. W. Lee, S. J. Sim, S. M. Cho, J. Lee, *Biosens. Bioelectron.* **2005**, *20*, 1422.

[42] E. Mauriz, M. C. García-Fernández, L. M. Lechuga, *TrAC-Trends Anal. Chem.* **2016**, *79*, 191.

[43] W. C. Tsai, I. C. Li, *Sensors Actuators, B Chem.* **2009**, *136*, 8.

[44] S. Sam, L. Touahir, J. Salvador Andresa, P. Allongue, J. N. Chazalviel, A. C. Gouget-Laemmel, C. H. De Villeneuve, A. Moraillon, F. Ozanam, N. Gabouze, S. Djebbar, *Langmuir* **2010**, *26*, 809.

[45] N. J. de Mol, M. J. E. Fischer, *Life Sci.* **2010**, 255.

[46] D. Blasi, L. Sarcina, A. Tricase, A. Stefanachi, F. Leonetti, D. Alberga, G. F. Mangiatordi, K. Manoli, G. Scamarcio, R. A. Picca, L. Torsi, *ACS Omega* **2020**, *5*, 16762.

[47] L. Sarcina, L. Torsi, R. A. Picca, K. Manoli, E. Macchia, *Sensors* **2020**, *20*, 1.

[48] L. Liu, D. Deng, Y. Xing, S. Li, B. Yuan, J. Chen, N. Xia, *Electrochim. Acta* **2013**, *89*, 616.

[49] D. Yang, R. Kroe-Barrett, S. Singh, T. Laue, *Antibodies* **2019**, *8*, 24.

[50] V. Ball, J. J. Ramsden, *Biopolymers* **1998**, *46*, 489.

[51] Ö. Torun, I. Hakki Boyaci, E. Temür, U. Tamer, *Biosens. Bioelectron.* **2012**, *37*, 53.

[52] R. B. M. Schasfoort, in *Handbook Of Surface Plasmon Resonance*, Royal Society Of Chemistry, London, UK **2017**, pp. 1–26.

[53] T. Verbić, Z. Dorkó, G. Horvai, *Rev. Roum. Chim.* **2013**, *58*, 569.

[54] K. Danzer, *Fresenius. J. Anal. Chem.* **2001**, *369*, 397.

[55] F. C. Dudak, I. H. Boyaci, *Biotechnol. J.* **2009**, *4*, 1003.

[56] P. D. Skottrup, M. Nicolaisen, A. F. Justesen, *Biosens. Bioelectron.* **2008**, *24*, 339.

[57] H. Baccar, M. B. Mejri, I. Hafaiedh, T. Ktari, M. Aouni, A. Abdelghani, *Talanta* **2010**, *82*, 810.

[58] P. Leonard, S. Hearty, J. Quinn, R. O'Kennedy, *Biosens. Bioelectron.* **2004**, *19*, 1331.

[59] L. De La Fuente, E. Montanes, Y. Meng, Y. Li, T. J. Burr, H. C. Hoch, M. Wu, *Appl. Environ. Microbiol.* **2007**, *73*, 2690.

[60] Y. Tang, R. Memaugh, X. Zeng, *Anal. Chem.* **2006**, *78*, 1841.

[61] M. B. Medina, L. Van Houten, P. H. Cooke, S. I. Tu, *Biotechnol. Tech.* **1997**, *11*, 173.

[62] E. Rostova, C. Ben Adiba, G. Dietler, S. K. Sekatskii, *Biosensors* **2016**, *6*, 52.